

# Pressure dependence of charge distribution along TCNQ columns in Cs<sub>2</sub>TCNQ<sub>3</sub>

journal or publication title	Journal of the Physical Society of Japan
volume	72
number	7
page range	1784-1788
year	2003-07
URL	<a href="http://hdl.handle.net/2298/10530">http://hdl.handle.net/2298/10530</a>

doi: 10.1143/JPSJ.72.1784

# Pressure Dependence of Charge Distribution along TCNQ Columns in Cs<sub>2</sub>TCNQ<sub>3</sub>

Hasanudin<sup>1\*</sup>, Noritaka KURODA<sup>1,2</sup>, Tomoko KAGAYAMA<sup>1</sup>,  
Toyonari SUGIMOTO<sup>3</sup>, Michihiro KOBAYASHI<sup>2,4</sup>

<sup>1</sup>*Department of Mechanical Engineering and Materials Science, Faculty of Engineering,  
Kumamoto University, Kumamoto 860-8555, Japan*

<sup>2</sup>*CREST, Japan Science and Technology Corporation, Kawaguchi 332-0012, Japan*

<sup>3</sup>*Research Institute for Advanced Science and Technology,  
Osaka Prefecture University, Sakai 599-8570, Japan*

*Graduate School of Engineering Science, Osaka University, Osaka 560-8531, Japan*

(Received )

## ABSTRACT

Pressure dependence of the charge distribution along the columns of tetracyanoquinodimethane (TCNQ) molecules in Cs<sub>2</sub>TCNQ<sub>3</sub>, which is a semiconducting 1/3-filled Hubbard system with the optical energy gap of 0.3 eV at ambient conditions, has been studied by the infrared and visible absorption experiments. An electronic phase transition is found to occur at around 3.5 GPa, in accordance with the previously reported insulator-to-metal transition. Our result suggests that this phase transition accompanies a symmetry change in the relative position of the TCNQ<sup>-</sup> radical molecules sandwiching the TCNQ<sup>0</sup> neutral molecule. In addition, the  $\pi^*$  electrons, which are localized on the TCNQ<sup>-</sup> molecules in the low-pressure phase, are delocalized significantly in the high-pressure phase. However, in the high-pressure phase the  $\pi^*$  electrons still maintain the localizing character. The charge-transfer degree of the neutral-like and radical-like molecules of the high-pressure phase is estimated to be  $\rho = 0.46-0.50$  and  $0.75-0.77$ , respectively.

Keywords: TCNQ compounds, insulator to metal transition, high pressure, infrared

-----  
\*On-leave from Faculty of Engineering, Tanjungpura University, Pontianak 78124,  
Indonesia.

Corresponding author: Hasanudin, Department of Mechanical Engineering and Materials Science,  
Faculty of Engineering, Kumamoto University, Kurokami 2-39-1, Kumamoto 860-8555, Japan  
Tel: +81-96-342-3727 Fax: +81-96-342-3710 e-mail: hasan@msre.kumamoto-u.ac.jp

## 1. Introduction

The electronic properties of the TCNQ complexes constructed from quasi-one-dimensional columns of TCNQ molecules as the electron acceptor and separately stacked columns of the donor atoms, largely depend on how the excess electrons are distributed over the  $\pi^*$  orbits of the TCNQ molecules. The distribution of the excess electrons is expressed in terms of the charge-transfer degree  $\rho$  of individual TCNQ molecules. If  $\rho$  is partial ( $\rho < 1$ ) like in the case of TTF-TCNQ, the compound usually exhibits a high electrical conductivity, whereas in the case of the complete charge transfer ( $\rho = 1$ ) like that of K-TCNQ and other alkali metal salts, the compound exhibits a comparatively low conductivity. To evaluate  $\rho$  the independent experiment is required since in many cases the value of  $\rho$  can not simply be presumed from the conductivity. The Raman spectroscopy, for instance, has been proved to be a good tool for determining  $\rho$ <sup>1)</sup>. Recently the infrared spectroscopy on the molecular vibration has been successfully applied to the study of the variation of the charge distribution upon a pressure-induced neutral-ionic phase transition<sup>2)</sup>.

This work deals with  $\text{Cs}_2\text{TCNQ}_3$ , a compound with the cation/anion ratio of 2:3. The charge-transfer degree is expected to be partial, that is,  $\rho = 2/3$ , if the  $\pi^*$  electrons are distributed uniformly over the columnar TCNQ molecules. Nevertheless, the room temperature electrical conductivity of this compound,  $\sim 10^{-3} \Omega^{-1}\text{cm}^{-1}$  (ref.3), is only slightly higher than that of the insulating 1:1 TCNQ salts. This is because the  $\pi^*$  electrons are not uniformly distributed, but are localized on certain sites forming TCNQ<sup>-</sup> radicals. Viewed from the crystal structure, the stack itself appears to be made of repetitive trimeric units, with two dimerized radical molecules (TCNQ<sup>-</sup>) sandwiching a neutral molecule (TCNQ<sup>0</sup>)<sup>4)</sup>. The most recently reported linearly polarized absorption measurement in the mid-infrared region, which provides clear and direct information on the absorption edge in this substance, suggests the presence of the optical energy gap of  $\sim 0.3$  eV<sup>5)</sup>. This fairly large energy gap gives the evidence of the localization of electrons on the radical molecules. The physical scheme of this situation is given in terms of the Hubbard model that the on-site Coulomb repulsion energy  $U$  (1.2 eV) is sufficiently large compared to the transfer integral  $t$  (0.11 eV) between the adjacent molecules on the stack<sup>6)</sup>.

Two charge-transfer bands, one between radical and neutral TCNQ molecules, and the other between radicals themselves, appear in the optical absorption/reflection spectrum in the visible region<sup>6,7)</sup>, reflecting the above-mentioned localization scheme. This is also confirmed from the characteristics of the molecular vibration modes observed by the infrared spectroscopy. In the infrared spectra, the molecular vibration modes appear as the superposition of those belonging to the neutral and radical molecules<sup>6,8)</sup>. The weighted average analyses on several vibration modes give the charge-transfer degrees  $\rho$  to be 0 and 1<sup>9)</sup> or 0.14 and 0.93<sup>8)</sup> for the neutral and radical molecules, respectively.

A pressure-induced insulator-to-metal transition has been observed by Matsuzaki through the

high-pressure electrical resistivity measurements in the present substance<sup>10)</sup>. The electrical resistivity decreases gradually with increasing pressure up to 2 GPa. When pressure exceeds 2 GPa, the resistivity abruptly decreases, and at around 4 GPa it becomes four orders of magnitude smaller than the value at the ambient pressure. The result of the subsequent Raman scattering measurement by Matsuzaki *et al.* shows that the C=C stretching mode consists of two lines, one belonging to TCNQ<sup>0</sup> and the other to TCNQ<sup>-</sup> at the ambient pressure<sup>11)</sup>. At high pressures those two lines tend to be combined into a single line, suggesting that the  $\pi^*$  electrons are delocalized from TCNQ<sup>-</sup> to become highly conducting. According to our recent infrared experiment, however, the Drude tail is not observed and the energy gap remains unclosed throughout the transition<sup>5)</sup>. Consequently the electronic structure of this metallic state might be considerably different from that of an ordinary metal.

The purpose of this work is to study the electronic mechanism underlying the above mentioned phase transition in Cs<sub>2</sub>TCNQ<sub>3</sub>. We measure the pressure dependence of the infrared absorption due to molecular vibrations and of the visible absorption due to electronic transitions. On the basis of the results we discuss the changes in the distribution of electrons along the stack, the stack structure of TCNQ molecules and the electronic structure.

## 2. Experimental procedure

The Cs<sub>2</sub>TCNQ<sub>3</sub> salt is synthesized from the reaction of TCNQ with an excess of CsI, and the single crystals of this material are obtained by the recrystallization from acetonitrile-ether solution. The as grown single crystals of Cs<sub>2</sub>TCNQ<sub>3</sub> are used as the samples. The pressure is generated using a diamond anvil cell (DAC). The optical absorption spectrum is measured using two microscope-spectrometer systems, one covering the spectral region from mid-infrared to near-infrared with a FT-IR spectrometer and the other one from near-infrared to visible with a multichannel polychromator equipped with a CCD detector. The ruby fluorescence method is used for calibrating the pressure. The linearly polarized spectra are measured at the ambient pressure to clarify the anisotropy of the vibrational and electronic transitions. Only the unpolarized spectra are measured in the high-pressure experiments since the film polarizer suitable for the measurement with DAC in the infrared region is unavailable.

In the measurement of the high-pressure optical absorption in the infrared region, one will encounter the problem that the strong absorption by the pressure-transmitting medium sometimes obscures the absorption due to the sample in a certain spectral region. For this reason two different pressure-transmitting media, flourinert (FC-40) and daphne oil, are used properly in the present experiment.

### 3. Results

Figure 1 shows the polarized absorption spectra at the ambient pressure and room temperature in the infrared region for the linear polarizations  $E//a$  and  $E//b$ , where  $E$  is the electric field of light and  $a$  and  $b$  are the crystal axes. The light is incident normal to the  $(ab)$  plane of the sample with a thickness of  $\sim 5 \mu\text{m}$ . Here the intensity of optical absorption is expressed by the absorbance defined as  $A = -\log_{10} T$ , where  $T$  is the transmittance. Our result demonstrates that the spectrum is contrasting in intensity between the two polarizations. For both polarizations the overall spectra correspond very well in the spectral position to previously reported results<sup>6,8)</sup>. In addition to the normally infrared active modes, very strong electron-molecular-vibration (EMV) coupled modes  $a_g$ 's of TCNQ molecules are observed at 1184, 1580, 2189  $\text{cm}^{-1}$  and so on for the  $E//b$  polarization<sup>8)</sup>. Furthermore, an intragap electronic absorption band<sup>5)</sup>, of which the origin is unidentified at present, spreads from 1100  $\text{cm}^{-1}$  beyond 1700  $\text{cm}^{-1}$  with a peak at around 1450  $\text{cm}^{-1}$  (0.17 eV). For  $E//a$ , on the other hand, the EMV modes have much lower intensities, reflecting that the radical-to-neutral and/or the inter-radical charge-transfer transitions responsible for the EMV modes are much weaker for  $E//a$  than  $E//b$ .

Figure 2 shows the unpolarized absorption spectra in the region of the C-CN stretching vibration of TCNQ molecules at several pressures. The thickness of the sample is  $\sim 10 \mu\text{m}$ , and the daphne oil is used as the pressure-transmitting medium. The features observed at 1205 and 1211  $\text{cm}^{-1}$  at the ambient pressure are the infrared active  $b_{2u}(v_{36})$  modes belonging to the neutral and radical molecules, respectively, whereas the one at 1184  $\text{cm}^{-1}$  is the aforementioned EMV coupled mode. We note that the spectrum at the ambient pressure resembles the one observed for  $E//a$  in Fig. 1 well.

A consideration should be made to understand the unpolarized spectrum obtained from the measurement using the diamond anvil cell. The actual quantity measured in this measurement is the light transmitted through the sample. In the unpolarized measurement, we measure the average of  $E//a$  and  $E//b$  components of the transmitted light. The weak absorption for  $E//a$  gives rise to a large transmission of the  $E//a$  component. For  $E//b$  polarization, however, the absorption due to molecular vibration is very strong. In addition, the continuous background due to the intragap electronic transition amounts to 0.5 in the absorbance for  $E//b$ , so that the  $E//b$  component of the transmitted light becomes very weak. In this situation, the transmittance is dominated by the light of  $E//a$  polarization, and therefore the absorbance spectrum reflects the properties of the  $E//a$  spectrum rather than the  $E//b$  spectrum. This is also true for the spectra observed under pressure. It is likely from Fig. 2 that the electronic absorption band is intensified by the application of pressure.

The two features at 1205 and 1211  $\text{cm}^{-1}$  show a blue shift with increasing pressure, while increasing their frequency spacing. At around 3.6 GPa they abruptly displace toward each other about half the way of the frequency spacing, and above 3.6 GPa they keep blue-shifting with the same rates. On the other hand, the frequency of the EMV coupled mode remains almost unchanged

under high pressures. The pressure dependence of the frequency of those modes is shown in Fig. 3. Interestingly, the intensity of the EMV mode depends very much on pressure as plotted in Fig. 4. It is intensified with increasing pressure; when pressure exceeds 3 GPa it turns to diminish to disappear at around 3.6 GPa.

Figure 5 shows the unpolarized spectra in the region of the C-H stretching vibration at several pressures. The thickness of the sample is also  $\sim 10$   $\mu\text{m}$ , but the fluorinert (FC-40) is used as the pressure-transmitting medium. The modes observed at 3038 and 3054  $\text{cm}^{-1}$  at the ambient pressure are  $b_{2u}(v_{18})$  mode belonging to neutral<sup>12)</sup> and radical<sup>13)</sup> molecules respectively. They are blue-shifted with increasing pressure while slightly reducing their frequency spacing. When pressure exceeds 3 GPa, the mode belonging to the radical molecules abruptly displaces toward the lower frequency side so that the frequency spacing decreases. When pressure increases further they recover blue-shifting while maintaining their spacing. The pressure dependencies of the frequency of these modes are shown in Fig. 6.

We have intended to observe other modes such as C=C and C=N vibrations, but failed because the absorption due to the diamond anvils and pressure-transmitting medium is very strong in the relevant spectral regions.

As already mentioned, only the weak bands, i.e., the bands that appear in the  $E//a$  polarization, can be observed in the unpolarized absorption measurement. Alternately, the strong bands are expected to be observed in the reflection spectrum. Thus to test the  $E//b$  spectrum in the high-pressure phase we have also made the measurement of the unpolarized infrared reflection with respect to the  $(ab)$  plane under high pressures. The results are shown in Fig. 7. It emerges that the EMV coupled modes are intensified with increasing pressure, and remain observable even at  $\sim 5.7$  GPa. It should be noted that although the EMV modes in  $E//b$  polarization are intensified at high pressures, they remain very weak in the unpolarized absorbance spectrum because of the reasons explained above. In our numerical simulation, it may provide an absorbance of the order of 0.02 in the high-pressure phase, consistent with the experimental spectrum shown in Fig. 2.

Figure 8 shows the unpolarized absorption spectra in the near-infrared to visible region at several pressures. The thickness of the sample is also  $\sim 10$   $\mu\text{m}$ , and the daphne oil is used as the pressure-transmitting medium. The linearly polarized absorption spectrum in this region is strongly anisotropic,<sup>7)</sup> similar to the case of molecular vibration spectrum in the infrared region. A very intense and broad absorption band, called B, due to the inter-radical electronic transition appears in  $E//b$  polarization. This band is already very intense at the lower bound, being  $\sim 1.1$  eV, of the spectral sensitivity of our CCD detector, and spreads up to 2.3 eV. In the  $E//a$  polarization this transition emerges as a weak band, which we call  $S_1$ , at 1.3 eV, followed by the comparatively intense band C due to the local excitation within radical molecules; the latter rises from 1.8 eV to have a peak at 2.2 eV. Hence, for the same reasons as the case of the unpolarized infrared absorption, only the band

$S_1$  and the low-energy part of the band C can be observed in the unpolarized spectrum, as seen in Fig. 8. With increasing pressure both bands are blue-shifted, while being intensified and broadened significantly. When pressure exceeds 3 GPa, the  $S_1$  band abruptly diminishes to disappear at 3.6 GPa. The pressure dependence of the integrated intensity of  $S_1$  is plotted in Fig. 4 along with the intensity of the infrared ( $1184 \text{ cm}^{-1}$ ) EMV band. We see that  $S_1$  behaves in a manner very similar to the EMV band. This fact shows that the  $S_1$  band is responsible mainly for the EMV coupling for the polarization  $E//a$ , as pointed out previously by the present authors<sup>14)</sup>.

#### 4. Discussion

The experimental results presented in the preceding section clearly show that a pressure-induced electronic phase transition occurs at around 3.6 GPa. The concomitant, large reduction of the frequency spacing between the neutral and radical modes of both  $b_{2u}(v_{36})$  and  $b_{2u}(v_{18})$  vibrations indicates that the  $\pi^*$  electrons of  $\text{TCNQ}^{-p}$  molecules are significantly delocalized from radical to neutral molecules, in agreement with the Raman scattering measurement by Matsuzaki<sup>11)</sup>. However, our observation of the EMV modes by the reflection measurement assures also that the  $\pi^*$  electrons maintain the localization character in the high-pressure phase.

A quantitative measure of the localization character of the  $\pi^*$  electrons is the charge-transfer degree of TCNQ molecules. Let the actual valence of neutral-like and radical-like TCNQ molecules be  $-\rho^N$  and  $-\rho^R$ , respectively. Then, since the frequency difference  $\Delta\nu$  of a given infrared mode between the radical-like and neutral-like molecules is known to vary nearly linearly to  $\rho^R - \rho^N$ <sup>9)</sup>, the following relationship is expected to hold to a good approximation at a pressure  $P$ :

$$\frac{\Delta\nu(P)}{\Delta\nu(0)} = \frac{\rho^R(P) - \rho^N(P)}{\rho^R(0) - \rho^N(0)}. \quad (1)$$

In the present substance, since there are 2 excess electrons for every three molecular sites, we have

$$2\rho^R(P) + \rho^N(P) = 2. \quad (2)$$

To obtain the values of  $\rho^N(P)$  and  $\rho^R(P)$ , the information on  $\rho^N(0)$  and  $\rho^R(0)$  is necessary. As previously mentioned, from the analysis of several infrared vibration modes the values 0 and 1<sup>9)</sup> and 0.14 and 0.93<sup>8)</sup> have been reported for  $\rho^N(0)$  and  $\rho^R(0)$ , respectively. The former set has been estimated by comparing the frequency of the C-N stretching modes in various TCNQ complexes, whereas the latter set has been deduced from an analysis taking several, different vibration modes into account. The results of the of the present experiment show that for the C-H stretching mode  $\Delta\nu$  changes from  $16.0 \text{ cm}^{-1}$  at the ambient pressure to  $4.9 \text{ cm}^{-1}$  at 3.6 GPa, giving  $\Delta\nu(P)/\Delta\nu(0) = 0.31$

for  $P \geq 3.6$  GPa. If  $\rho^N(0) = 0$  and  $\rho^R(0) = 1.0$  are employed with this value of  $\Delta v(P)/\Delta v(0)$ , eqs.(1) and (2) yield  $\rho^N(P) = 0.46$  and  $\rho^R(P) = 0.77$  in the high-pressure phase above 3.6 GPa. If  $\rho^N(0) = 0.14$  and  $\rho^R(0) = 0.93$  are employed we obtain  $\rho^N(P) = 0.50$  and  $\rho^R(P) = 0.75$  for the high-pressure phase. It is suggested that the radical-like molecules retain a high valence of 0.7 - 0.8 in the high-pressure phase. The C-CN stretching modes, on the other hand, can not be simply treated in the same way as the C-H stretching mode since  $\Delta v$  increases with pressure in the low-pressure phase. The origin should be considered to be different from the change in the charge-transfer degree.

The disappearance of the EMV coupled mode and the  $S_1$  band above 3.6 GPa is reminiscent of the temperature dependence of optical absorption in  $(NMe_4)_2TCNQ_3$ <sup>14,15</sup>, where Me denotes  $CH_3$ . The  $TCNQ^-$  molecules are not perfectly eclipsed but is slightly displaced from each other along the short molecular axis, i.e., the  $a$ -axis at moderate temperatures in  $(NMe_4)_2TCNQ_3$ , as well<sup>16</sup>. Consequently, the dipole moment of the charge transfer transition is not perfectly parallel to the  $b$ -axis but is slightly canted to have a weak component along the  $a$ -axis, and thus drives the  $S_1$  and EMV bands for the  $E//a$  polarization. As temperature is elevated the second order phase transition takes place at 338 K to have the  $TCNQ^-$  molecules be completely eclipsed<sup>17</sup>, so that above 338 K both the  $S_1$  and EMV bands disappear for  $E//a$ . In this analogy, the present experimental result suggests strongly that the radical-like  $TCNQ^{\cdot p}$  molecules are eclipsed in the high-pressure phase of  $Cs_2TCNQ_3$ .

## 5. Conclusions

Our experimental results have demonstrated that the pressure dependencies of the normally infrared active modes and the EMV modes complementarily provide the information on the changes in the intermolecular distribution of the  $\pi^*$  electrons upon the pressure-induced insulator-to-metal transition in  $Cs_2TCNQ_3$ . It turns out that, although the neutral  $TCNQ$  molecules are significantly charged and thus may give raise to a high electrical conductivity, the  $\pi^*$  electrons maintain the localizing, semiconducting character in the high pressure phase.

## Acknowledgements

This work was supported in part by the Grant-in-Aid for Scientific Research on Priority Areas (B) from the Japanese Ministry of Education, Science, Sports and Culture. The authors are grateful to Prof. K. Murata for providing us the purified daphne oil.



## References

1. S. Matsuzaki, R Kuwata, K. Toyoda, *Solid State Commun.* **33** (1980) 403.
2. L. Farina, A. Brillante, M. Masino, A. Girlando, *Phys. Rev. B* **64** (2001) 144.
3. J.S. Blakemore, J.E. Lane, D.A. Woodbury, *Phys. Rev. B* **18** (1978) 6797.
4. C.J. Fritchie, Jr., P. Arthur, Jr., *Acta Cryst.* **21** (1966) 139.
5. Hasanudin, T. Kagayama, N. Kuroda, T. Sugimoto, *Phys. Stat. Sol. (b)* **223** (2001) 337.
6. K. D. Cummings, D. B. Tanner, J. S. Miller, *Phys. Rev. B* **24** (1981) 24.
7. J. Tanaka, M. Tanaka, T. Kawai, T. Takabe, O. Maki, *Bull. Chem. Soc. Jpn.* **49** (1976) 2538.
8. Painelli, C. Pecile, A. Girlando, *Mol. Cryst. Liq. Cryst.*, **134** (1986) 1.
9. Chappel, J.S., Bloch, A.N., Bryden, W.A., Maxfield, M., Poehler, T.O., Cowan, D.O., *J. Am. Chem. Soc.* **103** (1981) 2442.
10. S. Matsuzaki, *Synth. Met.* **61** (1993) 207.
11. S. Matsuzaki, Y. Matsushita, M. Sano, *Solid State Commun.* **74** (1990) 1265.
12. T. Takenaka *Spectrochim. Acta* **27A** (1971) 1735.
13. M. Futamata, Y. Morioka, I. Nakagawa, *Spectrochim.* **39A** (1983) 515.
14. Hasanudin, N. Kuroda, T. Sugimoto, *Synth. Met.* **120** (2001) 1045.
15. N. Kuroda, Hasanudin, T. Sugimoto, K. Ueda, M. Kohama, N. Toyota, *Synth. Met.* **103** (1999) 2327.
16. K. Ueda, T. Sugimoto, S. Endo, N. Toyota, M. Kohama, K. Yamamoto, Y. Suenaga, H. Marimoto, T. Yamaguchi, M. Munakata, N. Hosoito, N. Kanehisa, Y. Shibamoto, and Y. Kai, *Chem. Phys. Lett.* **261** (1996) 295.
17. K. Yagi, H. Terauchi, N. Kuroda, K. Ueda, T. Sugimoto, *J. Phys. Soc. Jpn.* **68** (1999) 3770.

Figure caption.

Figure 1. Polarized infrared absorption spectra at room temperature.

Figure 2. Unpolarized infrared absorption spectra in the C-CN stretching region at several pressures.

Figure 3. Pressure dependencies of the position of the vibrational modes in the C-CN stretching region. The error bars indicate the width of the peaks.

Figure 4. Pressure dependencies of the intensity of  $S_1$  band and the EMV mode.

Figure 5. Unpolarized infrared absorption spectra in the C-H stretching region at several pressures.

Figure 6. Pressure dependencies of the position of the vibrational modes in the C-H stretching region. Frequency difference between neutral and radical vibration is on the inset.

Figure 7. Unpolarized infrared reflection spectrum at several pressures.

Figure 8. Unpolarized absorption spectra in the near infrared to visible region at several pressures.

Figure 1

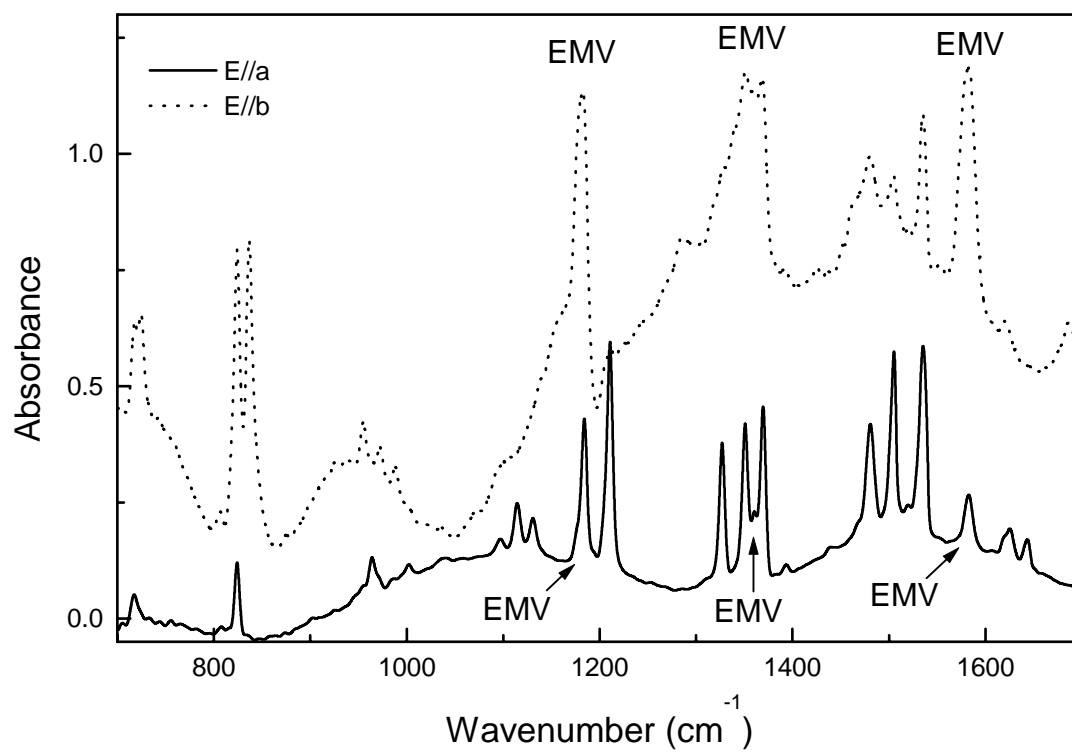


Figure 2.

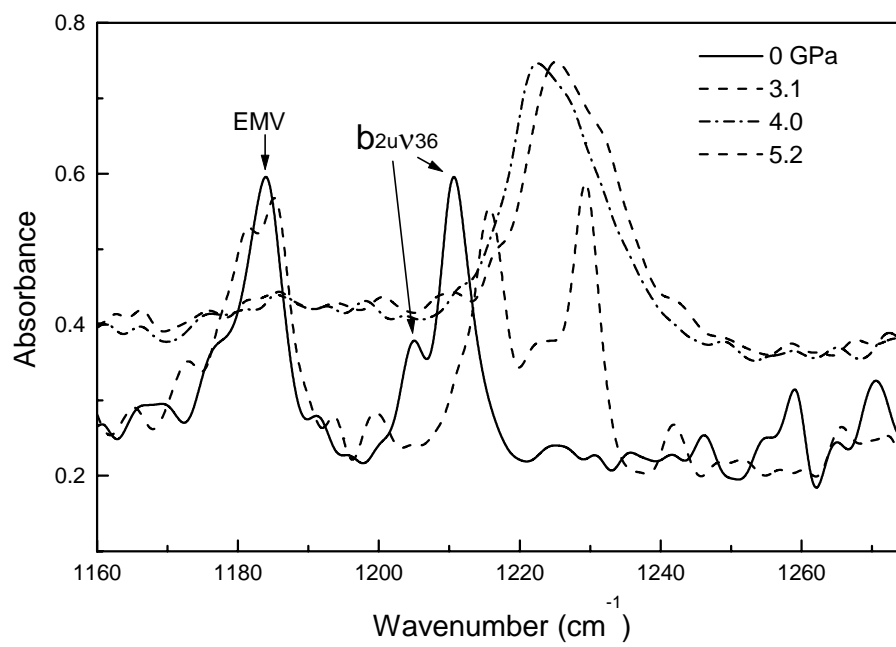


Figure 3.

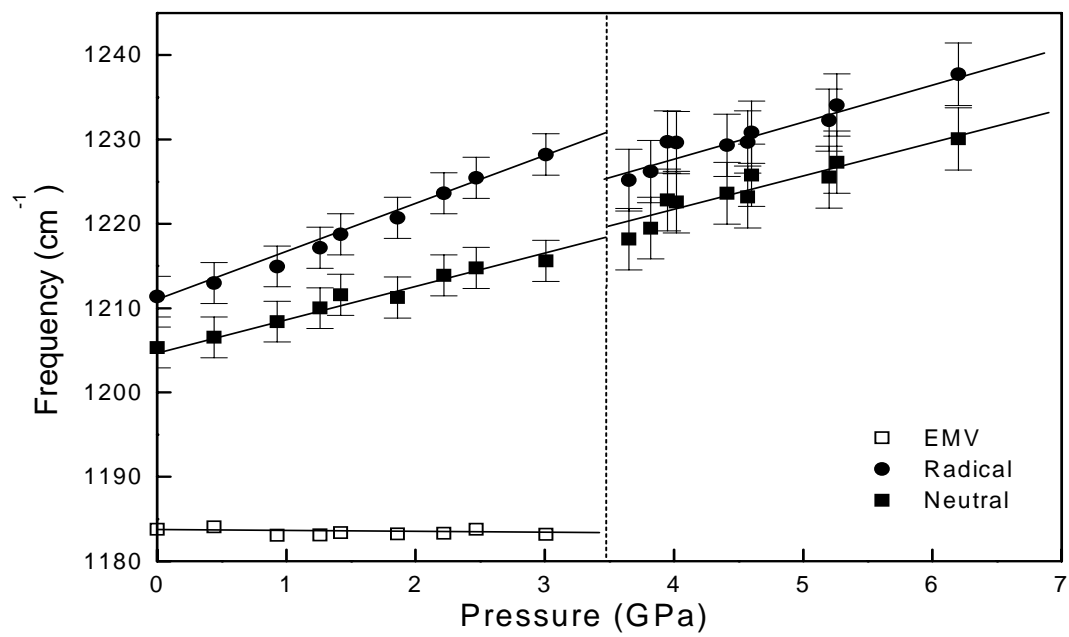


Figure 4.

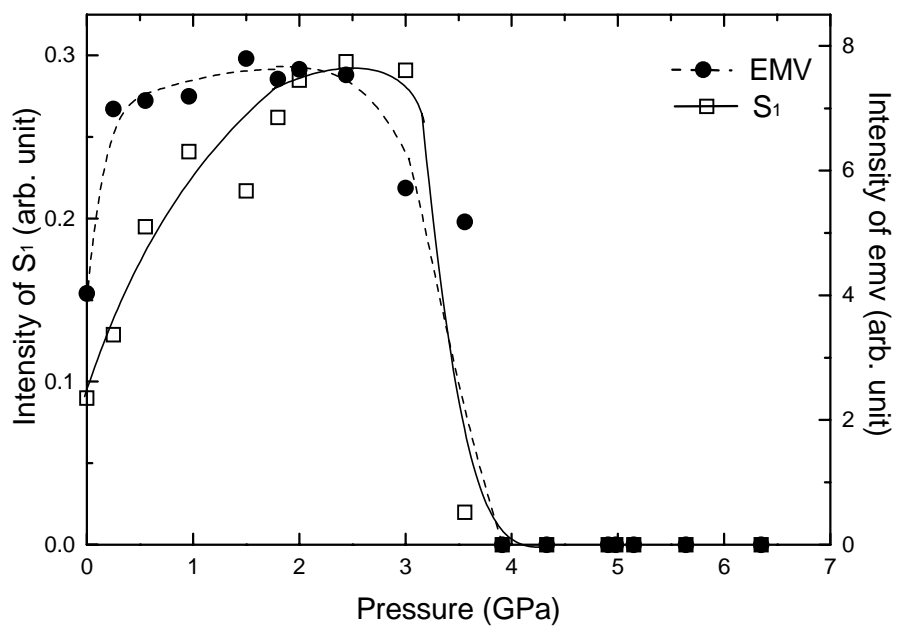


Figure 5.

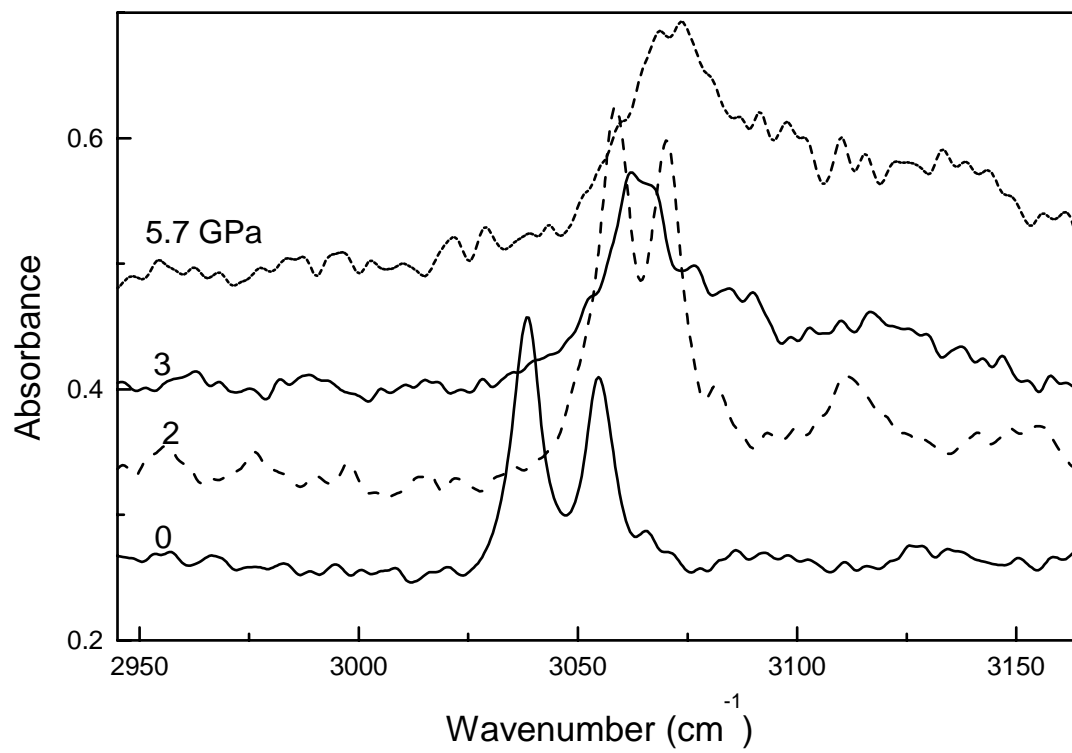


Figure 6.

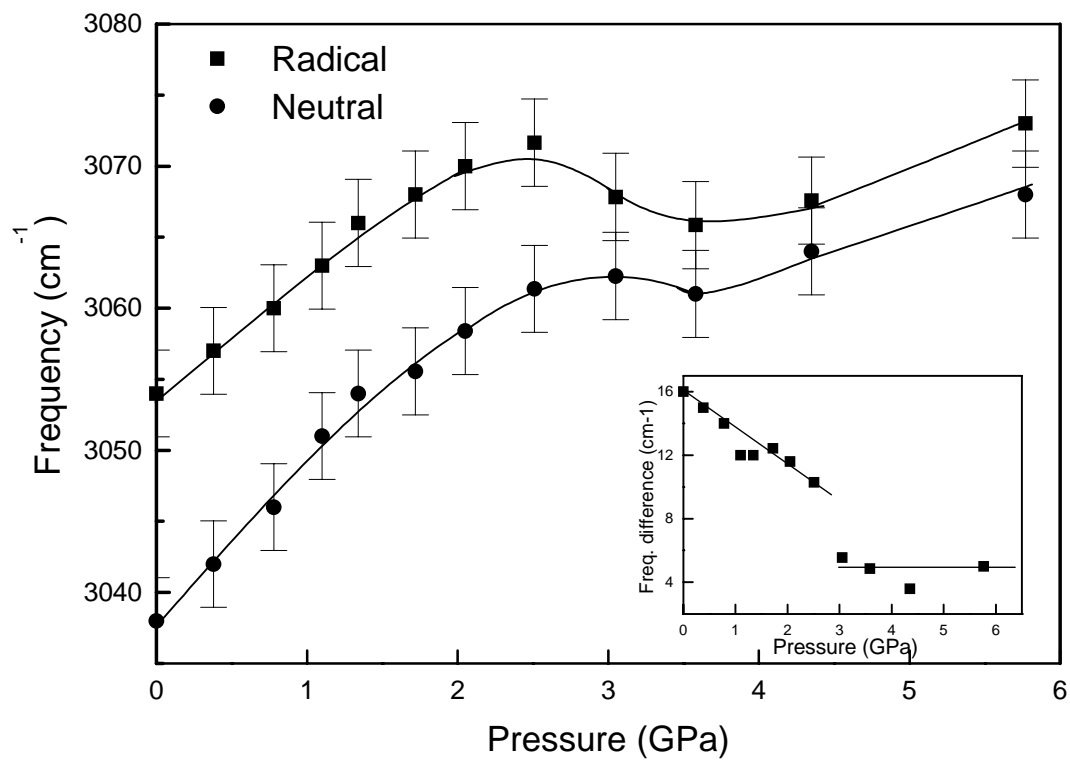




Figure 7.

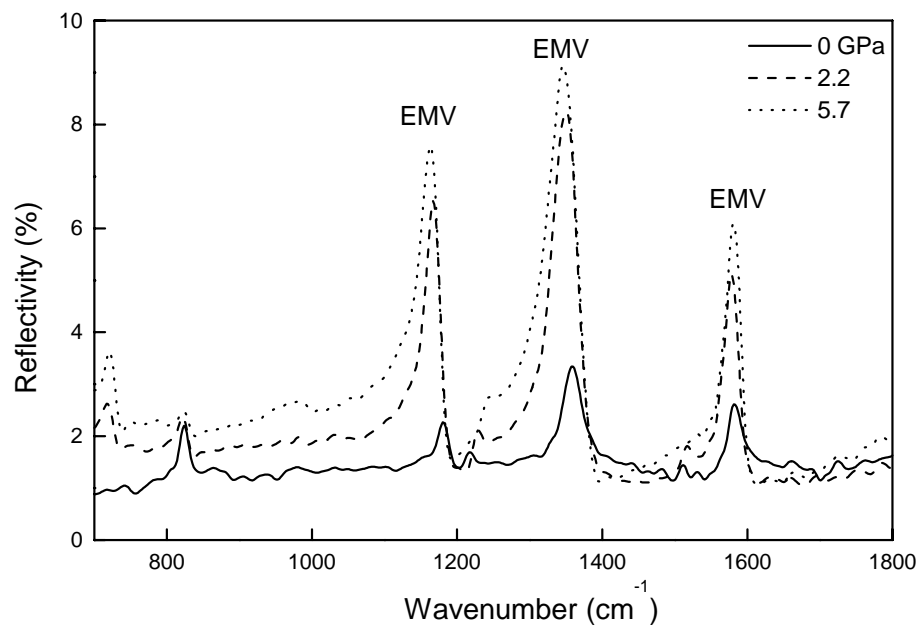


Figure 8.

